Springer

KSME

Journal of Mechanical Science and Technology 26 (5) (2012) 1311~1314
www.springerlink.com/content/1738-494x
DOI 10.1007/s12206-012-0329-3

Fractality in turbulence[†]

S. M. Muztaba Salim[*] and Franck Nicolleau

Sheffield Fluid Mechanics Group, Department of Mechanical Engineering, University of Sheffield, S13JD, United Kingdom

(Manuscript Received October 7, 2011; Revised January 31, 2012; Accepted February 22, 2012)

Abstract

Fractality, as we introduce it, is an attribute relating to any object or system where the existence of self-similar replication of the whole is present in any order and scale. This phenomenon can be realized in any turbulent flow due to the self-similar flow structures in its energy cascade. This intrinsic natural fractality is dominant in any turbulent flow. This paper reports the effect of a forced fractality externally superimposed on a turbulent flow in a circular wind tunnel on this natural fractality. The forced fractality was created by a set of fractal orifice plates. The time correlation and energy spectra showed that the forced fractality significantly excites the natural fractality and increases flow mixing. Simultaneously, we found that the fractal orifice plate is much more efficient than the classical orifice plate with equal flow area in terms of the flow mixing.

Keywords: Turbulence; Fractal; Hot-wire; Orifice; Wind tunnel

1. Introduction

The classical approach to generate turbulence in the laboratory is the so-called grid method [1-5], in which fluid flow is forced through a mesh grid to generate turbulence. The main feature of grid turbulence is that it produces single-length turbulence scales at any instant. These scales then break down into progressively smaller scales as functions of both time and space until the viscous dissipation becomes effective. On the other hand, the fractal method as we call it is a variation of the grid method, in which the classical meshed structure is replaced by another meshed structure in which the cells have a fractal as opposed to a uniform distribution [6]. This fractal mesh produces self-similar scales of different lengths at any instance, as shown by various researchers [7-10]. The attribute of different length scales generated by the fractal method from larger to smaller scales is what we refer to as fractality. Fractality can be realized more effectively from fractal objects found in nature such as cauliflowers. A small segment of a cauliflower has a self-similar shape statistically identical to the whole cauliflower. A careful dissection of this very segment reveals the self-similar shape of the whole cauliflower, and this dissection process can reach several iteration levels after which the fractality disappears. In mathematics, fractality is defined more rigidly, i.e., the self-similar attribute extends to infinite iteration levels, such as the Cantor or Mandelbrot sets [11].

In the case of the turbulence energy cascade, self-similar fractality can be realized in different turbulence length scales in the statistical sense. Although the fractality observed in the cascade process is limited to the homogeneous and isotropic Kolmogorov scale [12], which also happens to be the smallest scale, the spatial distribution of these smallest structures can also be related to the fractal distribution. This is more comprehensible when compared with the distribution of the stars in the dark sky. Interstellar gas, which follows a hierarchical and self-similar structure in a wide range of scales, has a fractal distribution as reported by Sánchez [13]. Likewise, the self-similar structures in the turbulence cascade validate our claim that turbulence is fractal by nature. Thus, a fundamental issue of whether this cascade can be manipulated from the smallest scale level rather than the largest scale level as caused by the grid method is raised. Another issue is the possible specific role of an external fractality in the internal fractality of turbulence, i.e., exciting the turbulence level or increasing the flow mixing, is also interesting to determine.

The present study has two main objectives. The first is to explore the external fractality effect on the internal fractality of turbulence, and the second is to develop a new kind of orifice plate in place of the classical circular orifice plate. The length of the largest scales in the turbulence cascade is well known to be often constrained by a characteristic length scale in many industrial flow applications. For instance, in the case of turbulent pipe flow, the length of the largest scale cannot exceed the pipe diameter, provided that the pipe has a constant diameter. The same goes for the case where an orifice plate is installed in the pipe, introducing significant changes in the flow dynamics. Behind the orifice plate, a substantial pressure

[*]Corresponding author. Tel.: +44 7835563051
E-mail address: sraboon.salim@sheffield.ac.uk
[†]This paper was presented at the AJK2011, Hamamatsu, Japan, July 2011. Recommended by Guest Editor Hyon Kook Myong and Associate Editor Yang Na.

deficit occurs and a weaker cascade process slows down the mixing, delaying the flow recovery. The orifice plate has gained overwhelming popularity as a differential flow meter over the last few decades owing to its comparatively low-maintenance cost, compared with many other existing flow meters. At the same time, the orifice plate is notoriously known to induce larger than required minimal pressure drop to measure the flow rate. Thus, the accumulated pressure drop by many orifice plates over the entire pipe length makes sustaining a constant flow rate very expensive. One way to speed up the flow recovery is to improve the flow mixing, perhaps by a forced energy cascade. In fact, Queiros-Conde and Vassilicos [14] found that a well-developed turbulence can be generated using fractal grids. Later, Seoud and Vassilicos [10] concluded that as much as three times of turbulence intensities can be produced using fractal grids compared with classical non-fractal grids. To resolve this problem from the engineering point of view, we proposed a fractal orifice plate and conducted hot-wire experiments to compare the time correlation and energy spectra between both the classical and fractal orifice plates of equal flow area.

2. Experimental setup

To address the issues raised in the latter part of the Introduction, we developed four fractal orifice plates, all variations of the classical circular orifice plate. Air flow forced through the orifice plates generated turbulence, and velocity data acquisition was performed by using hot-wire anemometry. The setup used in the experiment is given below.

2.1 Wind tunnel

The experiment was conducted in a bell-mouth [15] wind tunnel, as shown in Fig. 1. The 5 mm-thick polycarbonate tunnel had a length of 4400 mm and an inner diameter of 140.8 mm. The air was "sucked into" the test section through the bell-mouth by the electric motor fitted at the other end of the tunnel. The motor had a rating of 375 W and a speed of 2850 rpm. The flow exited through a control valve, which can be regulated to achieve the desired flow velocity in the tunnel. A vibration isolator is mounted between the fan and the wind tunnel to minimize motor-induced vibration that affects data acquisition.

The Reynolds number based on the pipe diameter was $Re_D = 3.98 \times 10^4$, and that based on the orifice flow diameter was $Re_d = 2.27 \times 10^4$. The inner diameter d_i of the classical circular orifice used in the experiment was 80 mm, and the outer diameter d_o was 140 mm. The diameter ratio between the orifice flow area and wind tunnel cross-section was $d/D = 80/140 = 0.57$.

Hot-wire measurements were performed in 14 downstream locations (hereafter referred to as "*Stations*"). Among these stations, the inlet station (*Station* 0), was 14.15*D* upstream of the orifice chamber, and the outlet station (*Station* 13) was 13*D* downstream of the orifice chamber. The remaining 12 stations were immediately behind the orifice chamber. The first station, *Station* 1, was 0.5*D* behind the orifice chamber followed by the remaining 11 stations. The distance between the two successive stations was 0.04*D*. All 14 stations were on the center axis of the tunnel.

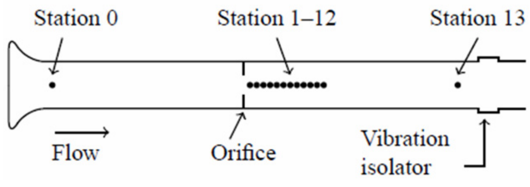

Fig. 1. Schematic of bell-mouth wind tunnel.

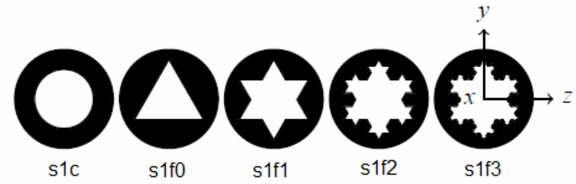

Fig. 2. Orifice plates with equivalent flow area (from left): reference classical circular orifice, s1c; and fractal orifice plates, s1f0–3, from the zeroth to third iteration.

2.2 Fractal orifice plates

The Koch set was adopted to design the fractal orifice plate, as shown in Fig. 1. A classical circular plate, *C*, with an inner diameter of 80 mm was used as the reference. The fractal orifice plates were carefully designed to maintain the same equivalent flow area as the reference classical plate. Four iteration levels from zero to three were used to devise four fractal orifice plates, s1f0–3. The equivalent flow areas of all the orifice plates enabled a direct comparison of the plates to deduce the fractal effects on the flow dynamics.

2.3 Hot-wire anemometer

A constant-temperature type hot-wire system manufactured by Dantec Dynamics (Model 54T30 miniCTA) and a hot-wire probe (Model 55P16) from the same manufacturer was used to collect the velocity data. The output signal from the anemometer was continuously analog. An analog-to-digital converter from National Instruments (Model PCI-6023E) was used to obtain the digital signal. This anemometer allowed a single input from the hot-wire probe and a single output to the analog-to-digital converter. The hot-wire probe was calibrated using a TSI 1125 calibrator and a Furness FC0510 micromanometer. The manometer was capable of measuring 2000 Pa to 0.001 Pa. The data acquisition error was handled carefully as instructed by Jørgensen [16].

2.4 Data acquisition and convergence test

Prior to the data collection during each measurement, hot-wire calibration was conducted to ensure reliable data. Each measurement was performed at a maximum frequency of 10 kHz. To determine the number of hot-wire sampling data for each point, a velocity convergence test was conducted at *Stations* 12 and 13. We randomly picked fractal orifice F2 for the convergence test. A total of 3 × 10^6 velocity data were measured. The convergence test was conducted in the following manner. We sequentially averaged the data points in 100 000 increments until all 3 × 10^6 data were covered. Finally, we constructed the "number of data vs. velocity curve". The fourth-order velocity fluctuation was found to be normalized by the plot of the mean velocity as a function of the number of data points from the convergence test. We decided that 1 × 10^6 data was sufficient to obtain the velocity information without jeopardizing the accuracy. The velocity measurement was limited to half of the tunnel diameter, assuming the flow had a radial symmetric profile given that it was a circular wind tunnel. The flow rate at each measurement was kept constant by regulating the control valve. The velocity time series data collected by the hot-wire measurement was used to construct time correlation curves and energy spectra for the data analysis. The spectra were calculated by performing Fourier transformation on the autocorrelation of velocity fluctuation. The notations used in the figures are *C* and *F* for the classical and fractal orifice plates, respectively. The indices used for *F* refer to the iteration levels from zero to three, a total of four iteration levels.

3. Results and discussion

Fig. 3 shows the characteristic time correlation with a trend of increasing signal memory as a function of the downstream location behind the orifice plate on the centerline. This finding is intuitively physical and can be compared with the analogy of a jet from an orifice plate. A jet expands as a function of time whereas the turbulence weakens, as in the case of this experiment. The classical orifice plate has a lower memory than all the fractal orifice plates, which introduce strong oscillation around the increasing trend, an indication of the fractal scaling effects on the flow dynamics.

Fig. 4 shows the energy spectra on the centerline behind the orifice plates as a function of the downstream location. The spectra were obtained by performing a Fourier transformation on the autocorrelation of velocity fluctuation. *Stations* 1, 6, and 11 clearly indicate that the spectra are developing. Although identical in form, the classical orifice plate has less energy than the fractal orifice plates. Based on the frequency, the spectra can be divided into three regimes until 1.5*D*, with regime 1 having a frequency range of 1–40 Hz; regime 2, 40–400 Hz; and regime 3, 400–10 000 Hz.

The first regime belongs to the lower frequency zone. The spectrum slope in this regime develops from -1 to -1/3 as a function of the downstream location, and this development can be observed until *Station* 6 corresponding to 1.5*D* downstream of the orifice plate. In the second regime, a sudden peak in the spectrum is observed. This peak can be attributed to the vortices shedding at the sharp edge of the orifice plate.

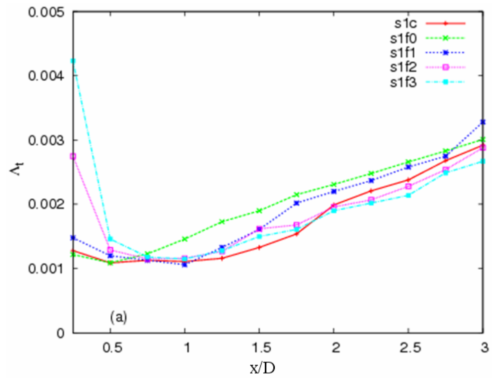

Fig. 3. Time correlation, Λ_t, as a function of the downstream location from the orifice plate on the centerline.

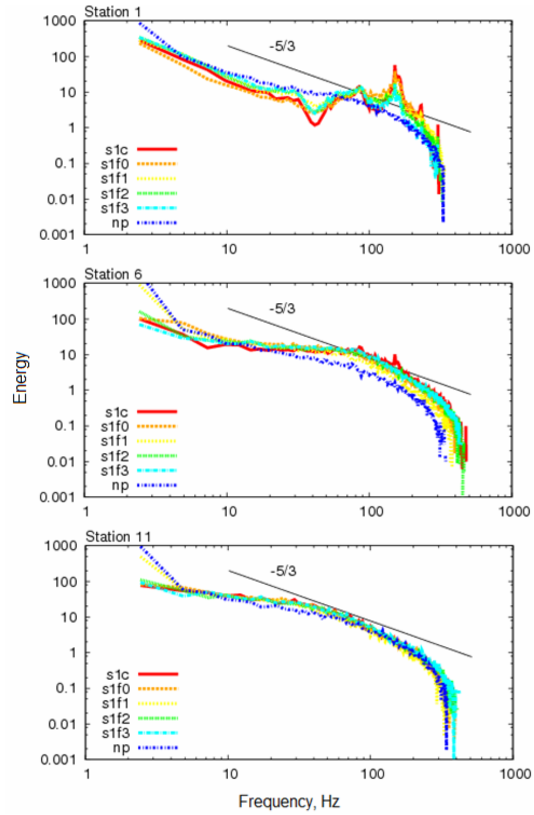

Fig. 4. Energy spectrum comparison of different orifice plates as a function of downstream locations on the centerline.

The vortex shedding has an intermediate frequency range matching this regime that vanishes at 1.5*D* downstream due to flow recovery in which the vortices lose their momentum and are diffused by the flow. The third regime, the largest of all three, exhibits the universal -5/3 slope pertaining to the classical Kolmogorov scales. This regime has the widest frequency range, which indicates good flow homogeneity. At the end of this regime, a sudden peak at 10 000 *Hz* is the hot-wire sampling frequency picked by the spectra. At *Station 6*, the dominant frequency shedding is still evidently pronounced behind the classical orifice plate (s1c), whereas the shedding is completely suppressed behind the fractal orifice plates (s1f0–3). This finding can be clearly associated with the fractal scaling. For the difference between any two successive fractal iteration levels, no information can be extracted. However, we speculate that as opposed to the single Reynolds number used in this paper, similar experiments using multiple Reynolds numbers may well elucidate the fractal scaling effects on the flow at each iteration level.

4. Conclusions

A turbulence study has been conducted following the fractal method to compare with the classical grid method usually employed. In the grid method, a meshed structure is used to create flow structures of a single length, and the energy cascade is generated as a function of time. In the fractal method, energy cascade formation is speeded up by creating structures with various length scales. The study had two objectives. One was to explore the effect of fractal forcing on the flow dynamics, and the other was to test the superiority of newly developed fractal orifice plates over the classical orifice plate in terms of flow mixing efficiency. Numerous hot-wire measurements were conducted to obtain the velocity time series behind the orifice plates, which were used for the data analysis.

The evolution of the time correlation and energy spectra as a function of the flow downstream of the orifice plates on the centerline shows that the fractal orifice plates are more efficient for flow mixing than the classical circular orifice plate. The natural cascade process of turbulent flow is highly susceptible to the external fractality imposed by the fractal orifice plate. The external fractality speeds up the formation of the cascade process at a higher rate than that created by the classical circular orifice plate.

Acknowledgment

This work was sponsored by Leverhulme Trust, London, and the Department of Mechanical Engineering, University of Sheffield, United Kingdom.

Nomenclature

D	: Pipe inner diameter, m
d_i	: Pipe inner diameter, m
d_0	: Pipe outer diameter, m
d	: Pipe diameter, m
W	: Power, W
β	: Wind tunnel cross sectional area, m^2
Λ_t	: Integral time scale
$s1c$	: Classical circular orifice plate
$s1f0$	: Fractal orifice plate at 0th iteration level
$s1f1$	: Fractal orifice plate at 1st iteration level
$s1f2$	: Fractal orifice plate at 2nd iteration level
$s1f3$	: Fractal orifice plate at 3rd iteration level

References

[1] M. S. Uberoi and S. Wallis, Effect of grid geometry on turbulence decay, *The Physics of Fluids*, 10 (6) (1967) 1216-1224.

[2] P. J. Zwart, R. Budwig and S. Tavoularis, Grid turbulence in compressible flow, *Experiments in Fluids*, 23 (1997) 520-522.

[3] R. Tresso and D. R. Munoz, Homogeneous, isotropic flow in grid generated turbulence, *Journal of Fluids Engineering*, ASME, 122 (2000) 51-56.

[4] S. M. M. Salim, T. Saga and N. Taniguchi, Experimental analysis of the control of turbulent intensity in a square channel, *JSME*, 10 (2004) 563-564.

[5] F. Murzyn and M. Bélorgey, Experimental investigation of the grid-generated turbulence features in a free surface flow, Experimental, *Thermal and Fluid Science*, 29 (2005) 925-935.

[6] M. Kearney, *Process intensification using engineered fluid transporting fractals*, AIChE Nat. Meeting (2003).

[7] F. Nicolleau, S. Salim and A. Nowakowski, Experimental study of turbulent pipe flow through a fractal plate, *J. Turbulence*, 12 (44) (2011) 1-20.

[8] C. J. Keylock, K. Nishimura, M. Nemoto and Y. Ito, The wake structure from fractal fences: Implications for the control of turbulence suspensions, *JSPS* (2005).

[9] D. Hurst and J. C. Vassilicos, Scalings and decay of fractal-generated turbulence, *Phys. Fluids*, 19 (2007) 035103.

[10] R. E. Seoud and J. C. Vassilicos, Dissipation and decay of fractal-generated turbulence, *Physics of Fluids*, 19 (2007) 105108.

[11] N. Lesmoire-Gordon, *Will rood and ralph edney, Introducing Fractal Geometry*, Icon Books, UK (2000).

[12] A. N. Kolomogorov, The local structure of turbulence in incompressible viscous fluid for very large Reynolds numbers, *C.R.Acad.Sci. U.R.S.S.*, 30 (1941) 301.

[13] N. Sánchez and E. J. Alfaro, The fractal distribution of HII regions in disk galaxies, *The Astrophysical Journal Supplement Series*, 178 (2008) 1-19.

[14] D. Queiros-Conde and J. C. Vassilicos, *Intermittency in turbulence and other dynamical systems*, Chapter: Turbulent wakes of 3-D fractal grids, Cambridge University Press, (2000).

[15] R. D. Mehta and P. Bradshaw, Design rules for small low speed wind tunnels, *The Aero. J. of the Royal Aero. Soc.*, Technical Notes (1979).

[16] F. Jørgensen, *How to measure turbulence with hotwire anemometers* - A practical guide. Dantec Dynamics (2002).

S. M. Muztaba Salim is a full-time graduate student at the University of Sheffield, United Kingdom. His research interests include experimental fluid dynamics, turbulence, flow control, etc.

F. Nicolleau is a full-time Senior Lecturer at the Department of Mechanical Engineering, University of Sheffield, United Kingdom. He is actively engaged in both computational and experimental turbulence research, flow control, fluidics, etc.